ORIGINAL PAPER

Effect of combined freezing with heat-moisture treatment (HMT) on the modification of in vitro digestibility, morphostructural, physicochemical, and thermal properties of Adzuki bean starch

Raphael Lucas Jacinto Almeida[1] · Newton Carlos Santos[1] · Iêda Letícia de Souza Ferreira[1] ·
Marcelo da Silva Pedro[1] · João Vítor Fonseca Feitoza[2] · Raphael da Silva Eduardo[3] · Vitória de Andrade Freire[3] ·
Tamires dos Santos Pereira[4] · Alison Bruno Borges de Sousa[4] · Artur Xavier Mesquita de Queiroga[5] ·
Pablícia Oliveira Galdino[6]

Abstract

The objective of the study was to evaluate the effect of freezing methods at -20 °C (S20) and -80 °C (S80) and liquid nitrogen at -196 °C (S196) applied to aduzki bean starch previously gelatinized by heat-moisture (HMT). It is characterized in terms of particle size distribution, functional properties, in vitro digestibility, specific surface area and thermal and morphostructural properties. Higher freezing rates (S196: 1.21 °C/min) resulted in a medium particle size (21–27 μm) and increased starch solubility (4.13–4.71%) and specific surface area due to rapid ice crystal formation. Freezing conditions had a significant impact ($p < 0.05$) on starch digestibility, with the lowest glycemic index obtained for S20 (68.36). X-ray diffraction (XRD) and Fourier-transform infrared spectroscopy (FT-IR) revealed that the freezing temperature did not modify the starch's crystalline form (type A) and did not identify new functional groups. However, relative crystallinity (19.03–21.88%) and IR 1022/945 (0.82–0.91) were reduced compared to the control (23.06%, 0.95, respectively). Different surface damage caused by freezing, such as pores and roughness on the surface, induced by HMT and intensified by the freezing method, was observed. Finally, gelatinized adzuki bean starch frozen at -196 °C (S196) demonstrated high functionality for use in the development of frozen starch-based foods. By combining freezing with HMT, we introduce a novel approach to starch modification that offers potential benefits compared to traditional methods. Utilizing combined thermal pre-treatments allows for rapid modification of native starch without chemical reagents, thereby facilitating large-scale application due to process simplicity.

Keywords Physical modification · Glycemic index · Gelatinization · Freezing rate

✉ Raphael Lucas Jacinto Almeida
    raphaelqindustrial@gmail.com

1   Department of Chemical Engineering, Federal University of Rio Grande do Norte, Natal, RN, Brazil

2   Department of Food Engineering, Federal University of Ceará, Fortaleza, CE, Brazil

3   Department of Chemical Engineering, Federal University of Campina Grande, Campina Grande-PB, Brazil

4   Department of Agroindustry, Federal Institute of Education, Science and Technology of Pernambuco, Belo Jardim, PE, Brazil

5   Department of Food Engineering, Rural Federal University of Pernambuco, Garanhuns, PE, Brazil

6   Department of Chemical, State University of Paraíba, Campina Grande-PB, Brazil

Introduction

Starch found in different parts of plants (seeds, fruits, stems, rhizomes, bulbs, and roots) can be isolated from various botanical sources, including cereals, legumes, and tubers [1]. Starch granules are microparticles with intercalated crystalline and amorphous regions, composed of amylose (α-1,4-glycosidic bonds) and amylopectin (α-1,6-glycosidic bonds) [2]. Legume seeds such as lentils, peas, soybeans, and beans contain, on average, about 45% starch, with bean starch content ranging from 30 to 60% [3]. Shi et al. [4] assessed the nutritional composition of 17 varieties of Chinese adzuki beans (*Vigna umbellata*) and reported that the total starch content ranged from 44.55 to 53.92%. The

extracted starch can be modified using various techniques to improve specific characteristics such as texture, water-holding capacity and particle size. One of the most commonly used methods in the food industry includes thermal methods, whether through the application of heat for cooking and sterilization or cold methods such as cooling and freezing for product preservation [5].

HMT has been used as a pre-treatment to modify starch for applications in bioplastics [6], noodles [7], nanocomposite films [8], sauces [9], rice cakes [10], and as a fat substitute in mayonnaise [11]. Overall, HMT can provide desirable physicochemical changes, as well as an increase in thermal stability and shear resistance [12]. Meanwhile, temperature variation is a central issue that cannot be ignored in the cold chain of the food industry. Thus, the structure of starch granules must be modified to improve the freeze-thaw stability of the gel to ensure high sensory quality and a long shelf life of starch-based frozen foods [13].

The most commonly used freezing methods in the food industry are refrigerator freezing, ultra-freezing, and liquid nitrogen freezing [14]. When employing the refrigerator method, heat is transferred via direct contact between the food and the cold wall. This method boasts the advantage of easy operation; however, it suffers from slow freezing speeds, leading to the formation of large ice crystals, which may potentially damage cellular tissues in frozen foods [15].

The application of liquid nitrogen involves direct contact with the product and is a method of rapid heat transfer with a large contact area, while the ultra-freezer has the advantage of faster freezing rates than domestic freezing and is slower than liquid nitrogen application [16].

Some studies have been conducted separately on heat-moisture treatment (HMT) and freezing techniques. For example, Gong et al. [17] applied HMT to modify adzuki bean starch, Li et al. [18] used HMT + electron beam irradiation on corn starch, Han et al. [19] applied HMT + ultrasound to pea starch, and Guo et al. [20] used HMT + microwave treatment on rice starch. Regarding freezing methods, there are examples such as Chen et al. [13] who investigated the freeze/thaw stability of corn starch gel with the application of pulsed electric field, Zhang et al. [21] studied freezing + ultrasound treatment of corn starch, and Wang et al. [22] examined freezing for potato starch. Given that most previous studies have focused on simple methods of starch modification, the application of combined freezing with HMT has remained relatively underexplored. Therefore, it is necessary to understand the behavior of gelatinized starch when subjected to freezing techniques, as this influences the structure of granules and their functional and nutritional properties, thus affecting the acceptability of the product. It is observed that after freezing, starch retrogradation occurs, which impacts the texture and stability of foods,

pharmaceutical products, and other colloidal systems, and modified starch has a higher water retention capacity [23]. The aim of this study was to assess the effect of freezing methods at different temperatures (-20, -80, and − 196 ºC) on HMT-gelatinized bean starch and characterize it regarding in vitro digestibility, thermal properties, functional properties, and morphostructural aspects.

Materials and methods

Materials

Adzuki beans (Coopernatural), sodium hydroxide (Neon), α-amylase from human salivary type XIII-A (EC 232-565-6) from Synth (São Paulo, Brazil), 3,5-dinitrosalicylic acid (DNS), ethyl alcohol, sodium metabisulfite, sodium acetate and acetic acid was purchased from Sigma Aldrich (Sigma Aldrich, St. Louis, MO, USA).

Starch isolation and heat-moisture gelatinization (HMT)

Initially, beans grains were soaked in a 0.5% sodium metabisulfite solution at a ratio of 1:2 (w/v) and maintained at a temperature of 7 °C for 72 h. After this soaking period, the grains were thoroughly rinsed with running water for 3 min. Next, the grains were placed in an industrial blender (Kohlbach, KM42A), and distilled water was added at a ratio of 1:2 (w/v). The grains were blended for 5 min. Following the blending step, the resulting suspension was filtered through an organza mesh to isolate the starch. This grinding and filtering process were repeated four more times. The liquid that passed through the mesh during filtration was collected and kept at a temperature of 7 °C. Every 12 h, the supernatant was removed, and this process was repeated five times, with the addition of 200 mL of distilled water at each interval. This process resulted in the preparation of a starch suspension for future use [24].

The gelatinization of the bean starch was carried out using the heat-moisture treatment (HMT) technique, where the starch (3 g) was adjusted to a moisture content of 20% and then sealed and heated at 110 ºC for 1 h in an electric oven (Philco, PFE48IP) with a power rating of 1500 W and dimensions of 31×55.5×44 cm [25].

Freezing treatments

For the freezing treatment of starch pastes with an initial moisture content of 85%, three different methods (S20, S80, and S196) were employed. The S20 method was produced by placing 100 g of starch on aluminum plates (15×2 cm)

with a thickness of 5.0 mm and leaving them in a commercial freezer (Eletrolux, FE27) at (-20±2ºC). The S80 method utilized an ultra-freezer (Solab, CL 580−80) at a temperature of -80±2ºC, while the S196 method used a freezer (GEA, LNF-6) with 300 g of liquid nitrogen at -196±3ºC [26, 27]. The temperature was confirmed using a type K thermocouple placed at the center of the plate and connected to the temperature recorder (Miaoguan, T10R-PT).

For the drying of the frozen starches, the same aluminum plates that were used for freezing were employed, and in the case of S196, the pellets with a diameter of 2–4 mm were arranged on the plates. Subsequently, they were placed in an air-circulating oven (Marconi, MA048) at 50ºC at a speed of 1.0 m s^{-1} for 690 min. After drying, the starches were ground in a disk mill (Botini, B55).

Determination of the size distribution of starch granules

The size distribution of bean starch granules was measured using dynamic light scattering (DLS) on a Zetasizer Nano-Zs equipped with a He-Ne laser (633 nm) and a digital correlator (ZEN3600). Measurements at a scattering angle of 173° were carried out at room temperature (25±2 °C) and pH 7.2 using a polystyrene cell, where starch was dispersed in distilled water at a proportion of 0.05% (w/v).

Solubility and swelling power

The 1% starch was placed in plastic tubes and stirred for 20 s, then subjected to temperatures of 40, 60 and 80 ºC in a thermostatic bath (LaborgLas, Alpha A12) for 30 min with intermittent vortexing. After that, it was cooled to 20 ºC and subsequently subjected to centrifugation at 3.000 rpm for 20 min. The separation process allowed the supernatant to be collected, which was subsequently dried at 120 ºC in an oven with air circulation (Marconi, MA048). The dry weights of the supernatant (P1), the pellet obtained post-centrifugation (P2) and the initial starch weight (P) were then used to calculate the swelling power and starch solubility, according to Eqs. 1 and 2 [28].

$$\text{Solubility } (\%) = \frac{P1}{P} \times 100 \tag{1}$$

$$\text{Swelling Power } \left(\text{gg}^{-1}\right) = \frac{P2 \times 100}{P \times (100 - solubility)} \tag{2}$$

Nitrogen gas adsorption for surface specific surface area determination

Starch (0.2 g) was deaerated and kept at 45 °C for 3 h, where nitrogen gas with a relative vapor pressure of 0.99 was adsorbed at a temperature of 77 K. Measurement of specific surface area was carried out. throughout the adsorption-desorption process and the results were expressed in units of square meters per gram (m^2 g^{-1}) using an automated gas analyzer (Micromeritics, ASAP2020) [29].

In vitro digestion of starch

The process was divided into a salivary digestion phase and a subsequent gastrointestinal phase. In the first stage, 2 g of starch were added to a solution of α-amylase (10 mg dissolved in 10 mL of 100 mmol L^{-1} sodium acetate buffer with pH 6.8) and agitated for 2 min at 37 °C. In the second stage, 0.5 mL of the supernatant from the previous stage was collected at various time intervals during digestion in the small intestine (at 5, 30, 60, 90, 120, 150, 170, and 200 min), then diluted with 2.5 mL of 95% ethanol [30]. Glucose concentrations were quantified using the reducing sugar assay method proposed by Miller [31], and the standard curve for starch digestion at different glucose concentrations was constructed following Eq. 3. Subsequently, the area under the curve (AUC) was calculated as described in Eq. 4, and the glycemic index (GI) was determined using Eq. 5.

$$C_t = C_\infty \times \left(1 - e^{-kt}\right) \tag{3}$$

$$AUC = C_\infty \left(t_f - t_0\right) - \left(\frac{C_\infty}{k}\right) \left[1 - \exp\left(-k\left(t_f - t_0\right)\right)\right] \tag{4}$$

$$GI = 39.71 + (0.549 \times HI) \tag{5}$$

C_t corresponds to starch digestibility at time t (min), C_∞ is the estimated final digestion percentage, k is the digestion rate coefficient, AUC represents the area under the curve, t_f signifies the final time (min), and t_0 denotes the initial time (min). The hydrolysis index (HI) was computed by dividing the area under the curve of the sample by the corresponding area for a reference food (parboiled rice).

Thermal analysis with differential scanning calorimetry (DSC)

The thermal transformation of native and treated bean starches was evaluated using a differential scanning calorimeter (Netzsch, DSC 214). Starch (3 mg) was mixed with water (6 μL) and sealed in an aluminum pan at 4 ºC for 24 h.

The pans with the starch were heated at a rate of 10ºC min^{-1} from 20ºC to 100ºC, under a nitrogen flow of 40 mL min^{-1}.

X-ray diffraction (XRD)

The diffractograms were generated using an X-ray diffractometer (Shimadzu, XRD-7000) equipped with Cu-Kα radiation filtered through nickel (wavelength of 0.15406 nm) operating at 15 mA and 35 kV. The data were collected at a scanning rate of 5º/min over a range of 10–35º (2θ). The crystallinity index of the starch granules was determined by calculating the ratio between the area of the peaks and the total area of the diffraction pattern, as per Eq. (6).

$$CI\,(\%) = \frac{T_a - A_{\mathrm{f}}}{T_a} \times 100 \tag{6}$$

CI is crystallinity index, such is the total area, and Af is the amorphous fraction area (g).

Fourier Transform Infrared Spectroscopy (FTIR)

The crystalline configurations of starch were ascertained using a Fourier transform infrared spectrometer (Agilent, Cary 630). The scanning wavelength range for the determination spanned from 650 to 4000 cm^{-1} with 256 scan cycles and a resolution of 4 cm^{-1}. Gaussian deconvolution and second-order derivation were employed to compute the ratio between the bands at IR1047/1022 cm^{-1} and IR1022/995 cm^{-1} [32].

Scanning electron microscopy (SEM)

Control and treated bean starch granules were visualized with a scanning electron microscope (Zeiss, Merlin Compact), where a thin layer of gold was applied to the samples and images were obtained at an accelerating voltage of 10 kV at magnification of ×3.000.

Statistical treatment

All analyzes were performed in triplicate for each treatment. Data were expressed as mean ± SD and analyzed by one-way analysis of variance (ANOVA) followed by Tukey's test using Statistica 7.0 software, where the difference was significant at $p < 0.05$.

Results and discussion

Freezing procedure and particle size distribution of starch

The curve showed that the freezing time was (S196: 4.8 ± 0.6 min; S80: 35 ± 2.4 min; S20: 93 ± 3.1 min), and the rates were (S196: 1.21 ºC/min; S80: 0.13 ºC/min; S20: 0.05 ºC/min) (Fig. 1A). Thus, according to the method used, the freezing rate is modified due to the time required for the starch to reach the chosen temperature, with the direct freezing method S196 using liquid nitrogen being the most efficient. Analyzing the particle size distribution of the control starch (Fig. 6B) and the frozen starches (Fig. 6C-E), it is noticeable that HMT followed by freezing significantly increased the particle diameter. The control starch presents a left-skewed distribution, indicating a tendency towards smaller values, while S196 shows a right-skewed distribution (Fig. 6E) with a tendency towards an increase in this parameter. The average sizes were (control: 6–18 μm; S20: 21–27 μm; S80: 38–42 μm; S196: 49–53 μm), and it was observed that the freezing rate affected the size of the ice crystals and the quality of the frozen foods. At lower freezing temperatures, more damage occurs because the starch structure is exposed, and the ice crystals formed rupture and break the bonds between amylose and amylopectin chains. Depending on the technique and temperature applied, there was greater agglomeration due to HMT, and with freezing, the ice crystals created permanently modified the structure [33]. The same was found by Yang et al. [34] for a temperature of -20ºC (26.36 μm). If freezing techniques were applied to native starch, what would occur is the compression of the granules due to the pressure exerted by the ice crystals [35]. Since the gelatinization treatment by HMT was applied earlier, the starch retrogradation, together with drying, prevented granule compression.

Solubility and swelling power

The solubility of starch (Table 1) showed a significant difference with the increase in temperature (40–80ºC) when the same formulation was observed, with higher values at 60ºC, highlighting the control sample (5.33%). When comparing the different formulations, it was noticed that freezing techniques led to a decrease in solubility when applied to gelatinized starch, even with the increase in temperature during solubilization. This effect was intensified mainly with the use of liquid nitrogen (S196) for freezing, with a minimum value of (4.13%). The increase in solubility may be related to structural differences and molecular properties, especially the weakening of hydrogen bonds between amylose and amylopectin chains [25]. According to Wei et al.
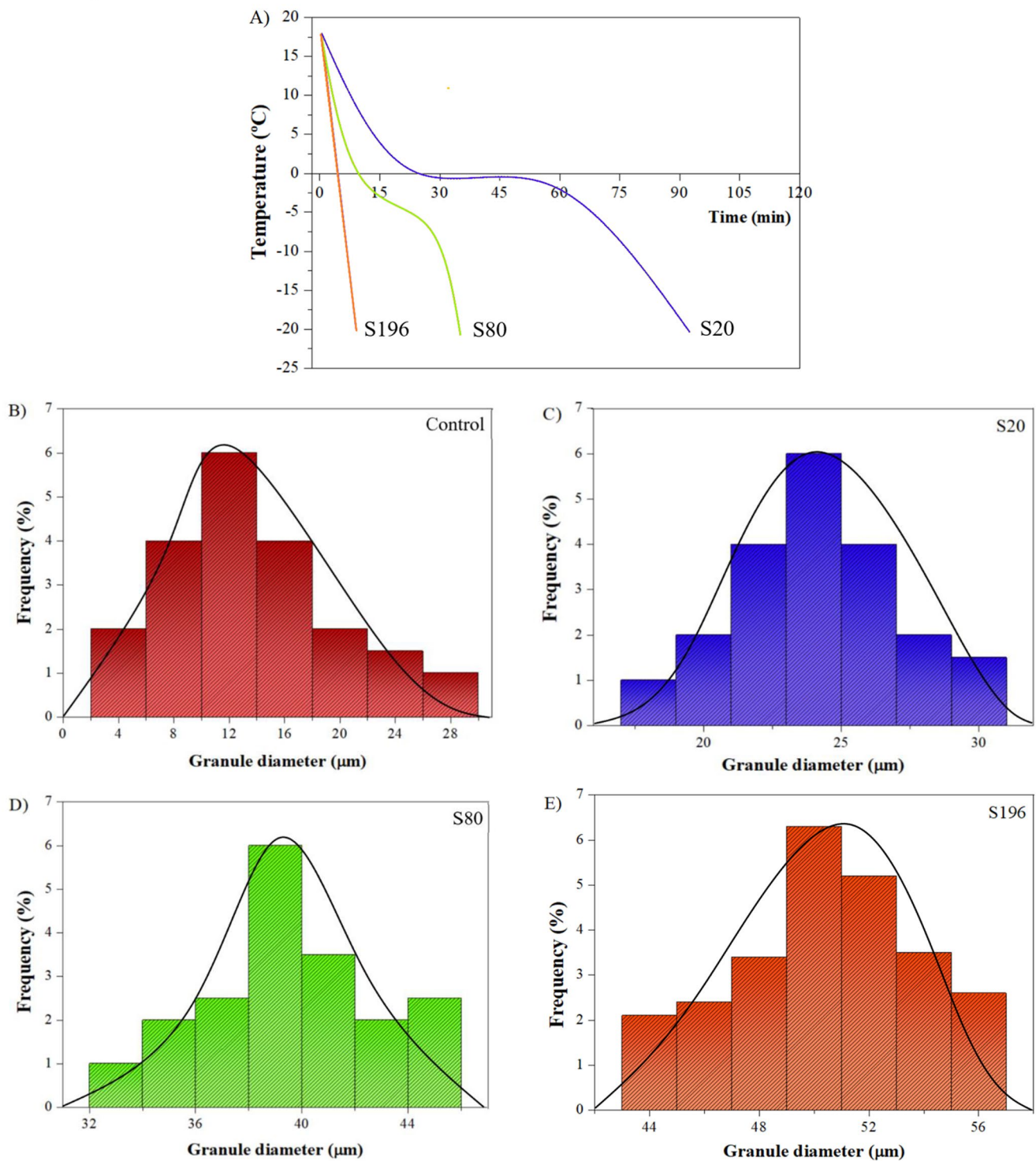
Fig. 1 Freezing process and size distribution. (**A**) Freezing curves of adzuki bean starch using 3 methods, (**B**) particle size of the control, (**C**) S20, (**D**) S80, and (**E**) S196. The control represents starch gelatinized by heat-moisture (HMT), S20 represents starch gelatinized by HMT and frozen at -20±2ºC, S80 represents starch gelatinized by HMT and frozen at -80±2ºC, and S196 represents starch gelatinized by HMT and frozen at -196±3ºC

Table 1 Effect of temperature on the solubility and swelling power of adzuki bean starch modified by HMT and freezing techniques

Parameters	Units	Control	S20	S80	S196
Solubility 40ºC	(%)	4.87 ± 0.06^{Ac}	4.69 ± 0.02^{Bc}	4.53 ± 0.05^{Cc}	4.13 ± 0.03^{Dc}
60ºC	(%)	5.01 ± 0.05^{Ab}	4.81 ± 0.05^{Bb}	4.62 ± 0.03^{Cb}	4.38 ± 0.02^{Db}
80ºC	(%)	5.33 ± 0.04^{Aa}	5.05 ± 0.03^{Ba}	4.97 ± 0.02^{Ca}	4.71 ± 0.04^{Da}
Swelling power 40ºC	g g^{-1}	4.11 ± 0.06^{Dc}	5.09 ± 0.07^{Cc}	5.82 ± 0.11^{Bc}	6.29 ± 0.05^{Ac}
60ºC	g g^{-1}	4.39 ± 0.05^{Db}	5.33 ± 0.25^{Cb}	6.05 ± 0.09^{Bb}	6.48 ± 0.02^{Ab}
80ºC	g g^{-1}	4.87 ± 0.07^{Da}	5.62 ± 0.17^{Ca}	6.47 ± 0.08^{Ba}	6.89 ± 0.04^{Aa}

Note Values are expressed (average ± standard deviation). Control is starch gelatinized by heat-moisture (HMT), S20 is starch gelatinized by HMT and frozen at -20 ± 2ºC, S80 is starch gelatinized by HMT and frozen at -80 ± 2ºC and S196 is starch gelatinized by HMT and frozen at -196 ± 3ºC. Different superscript capital letters indicate that there is a significant difference ($p < 0.05$) between the formulations at the same temperature and different superscript lowercase letters indicate that there is a significant difference ($p < 0.05$) for the same formulation at different temperatures

Table 2 Parameters of in vitro digestion, fitting to the first-order model, and glycemic index (GI) for frozen bean starch

Formulations	C_{∞} (%)	k (min^{-1})	R^2	χ^2
Control	26.93 ± 0.10^{D}	$1.50 \times 10^{-1} \pm 0.01^{A}$	0.942	0.805
S20	37.57 ± 0.19^{C}	$9.06 \times 10^{-2} \pm 0.02^{B}$	0.969	1.159
S80	41.86 ± 0.27^{B}	$8.89 \times 10^{-2} \pm 0.01^{C}$	0.988	0.687
S196	46.86 ± 0.31^{A}	$7.51 \times 10^{-2} \pm 0.04^{D}$	0.982	0.857
Formulations	**AUC**	**HI (%)**	**GI**	
Control	5786.46 ± 102.02^{D}	42.54 ± 2.49^{D}	63.06 ± 1.12^{D}	
S20	7099.32 ± 145.39^{C}	52.20 ± 1.56^{C}	68.36 ± 1.86^{C}	
S80	7899.54 ± 98.26^{B}	58.08 ± 1.77^{B}	71.59 ± 1.09^{B}	
S196	8748.03 ± 127.91^{A}	64.32 ± 2.34^{A}	75.02 ± 0.95^{A}	

Note Values are expressed (average ± standard deviation). Control is starch gelatinized by heat-moisture (HMT), S20 is starch gelatinized by HMT and frozen at -20 ± 2ºC, S80 is starch gelatinized by HMT and frozen at -80 ± 2ºC and S196 is starch gelatinized by HMT and frozen at -196 ± 3ºC. R^2: Coefficient of determination; χ^2: Chi-Square. C_{∞}: estimated percentage of final starch digestion; k: starch digestion rate coefficient; AUC: curve area; HI: hydrolysis index; GI: glycemic index. Different superscript capital letters indicate that there is a significant difference ($p < 0.05$) between the formulations

[27], the slower the freezing rate, the greater the increase in solubility, which is consistent with the data presented for S20 and S80.

Analyzing the swelling power, it was observed that the values increased when the temperature was raised from 40–80ºC and also increased in the order S196 > S80 > S20, with the highest value obtained for S196 at 80ºC (6.89 g g^{-1}). This can be justified as lower temperatures lead to the formation of smaller ice crystals, reducing the impact on starch structure. This results in a decrease in starch swelling power, although it remains higher than that of the control [36]. Yang et al. [26] observed the same behavior for non-previously gelatinized starch, with increasing values superior to the control.

The swelling power reflects the interactions between the crystalline and amorphous regions in starch granules, where low swelling power can be attributed to entanglement between amylose and amylopectin, hindering granule swelling [37]. According to Xu et al. [38], this parameter reflects starch hydration capacity, where hydrogen bonds tend to increase water retention.

Effect of freezing method on in vitro digestion of bean starch

Table 2; Fig. 2 present the results of in vitro digestibility with the adjustment of the first-order model. The initial value was approximately 15%, referring to the previously gelatinized starch (control) at time (T0). It is noticeable that freezing and thawing techniques facilitated enzyme diffusion, increasing starch digestion, reaching a maximum C∞ of 46.86% (S196). Almeida et al. [1] observed higher values (50.24% and 43.56%) when applying hydrothermal treatments (autoclaving and cooking) to red rice starch, respectively. However, for native starch, the value was 2.16%, lower than that found for the control subjected to HMT. Yang et al. [26] found that the digestibility of frozen starches without prior gelatinization did not show significant differences when temperatures up to -80ºC were used.

The k values ranged from 7.51×10^{-2} to 1.50×10^{-1}, depending on the formulations, where the values were inversely proportional to C∞, as expected, since the highest digestion rate was observed for the control, which showed stability at 60 min, while frozen samples reached stability at 120 min of hydrolysis (Fig. 2B-D). The initial enzymatic

Fig. 2 In vitro digestibility adjusted to the first order model of bean starch gelatinized by HMT and frozen by 3 different methods. (**A**) Control is starch gelatinized by heat-moisture (HMT), (**B**) S20 is starch gelatinized by HMT and frozen at -20 ± 2ºC, (**C**) S80 is starch gelatinized by HMT and frozen at -80 ± 2ºC and (**D**) S196 is starch gelatinized by HMT and frozen at -196 ± 3ºC
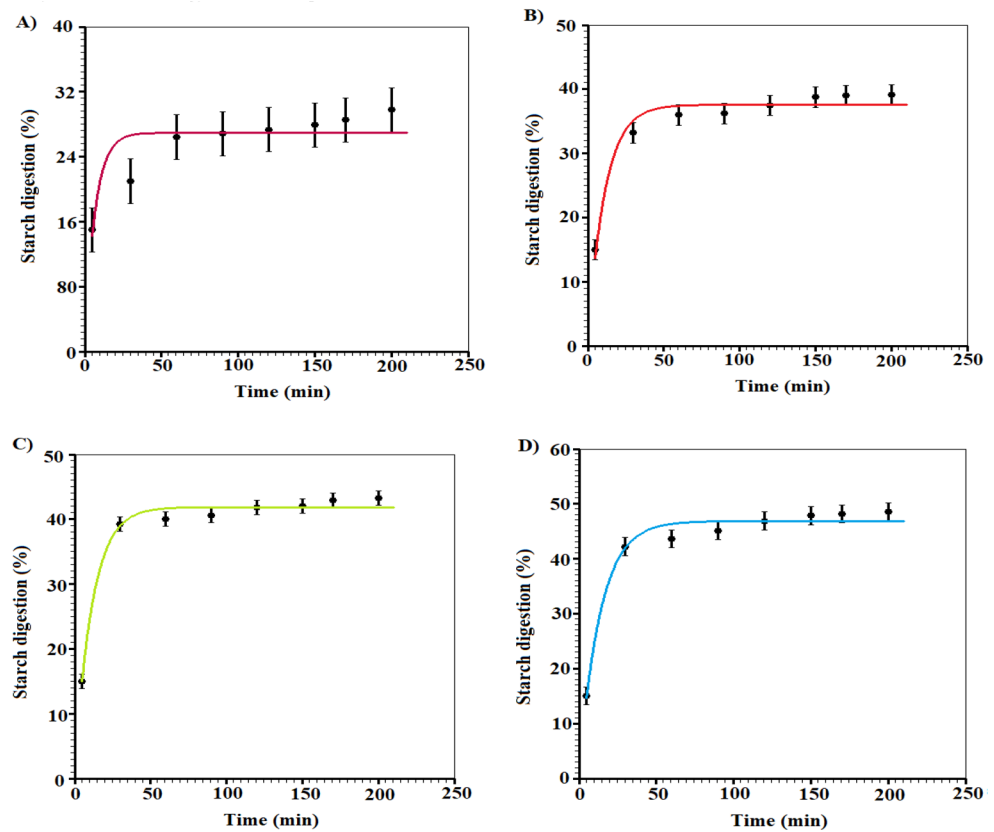
Table 3 Specific surface area and thermal parameters obtained by DSC of adzuki bean starch

Parameters	Units	Control	S20	S80	S196
Specific surface area	m^2 g^{-1}	0.58 ± 0.03^D	0.74 ± 0.03^C	0.92 ± 0.06^B	1.26 ± 0.04^A
Onset temperature (To)	°C	60.41 ± 0.11^A	60.03 ± 0.09^B	59.62 ± 0.11^C	59.17 ± 0.11^D
Peak temperature (Tp)	°C	67.17 ± 0.08^A	66.92 ± 0.08^B	66.14 ± 0.05^C	65.32 ± 0.12^D
Conclusion temperature (Tc)	°C	72.04 ± 0.12^A	71.51 ± 0.02^B	71.39 ± 0.07^C	71.14 ± 0.06^D
Enthalpy of gelatinization (ΔH)	(J g^{-1})	5.07 ± 0.03^C	5.55 ± 0.02^A	5.46 ± 0.01^B	5.20 ± 0.05^B

Note Values are expressed (average ± standard deviation). Control is starch gelatinized by heat-moisture (HMT), S20 is starch gelatinized by HMT and frozen at -20 ± 2ºC, S80 is starch gelatinized by HMT and frozen at -80 ± 2ºC and S196 is starch gelatinized by HMT and frozen at -196 ± 3ºC. Different superscript capital letters indicate that there is a significant difference ($p < 0.05$) between the formulations

hydrolysis process is relatively fast, resulting in a rapid increase in starch digestibility. As digestion progresses, starch molecules become more complex and difficult to decompose by digestive enzymes. This leads to a deceleration in the digestion rate and the gradual attainment of the peak digestibility [39].

Both formulations showed good fit with a coefficient of determination (R^2) greater than 0.94 and a chi-square value < 1.2, mainly for S80 with values of 0.988 and 0.687, respectively. The control presented the smallest area (5786.46) and consequently the lowest hydrolysis index (HI) (42.54), while frozen samples showed higher values, which were intensified by low temperatures, mainly with the direct method using liquid nitrogen (S196). All formulations showed a high glycemic index (GI > 60) due to HMT;

however, freezing techniques were effective in increasing this parameter, with the highest value observed for S196 (75.02).

Specific surface area and thermal parameters

A noticeable increase was observed for the formulations that underwent freezing treatment in terms of specific surface area (Table 3), with S196 standing out (1.26 m^2 g^{-1}). In this case, the temperature of -196ºC and the freezing time also influenced the porosity, as shown in the SEM (Sect. 3.7), where small empty spaces contributed to this parameter being elevated.

When particle porosity increases, it results in an increase in the specific surface area, often referred to as "internal
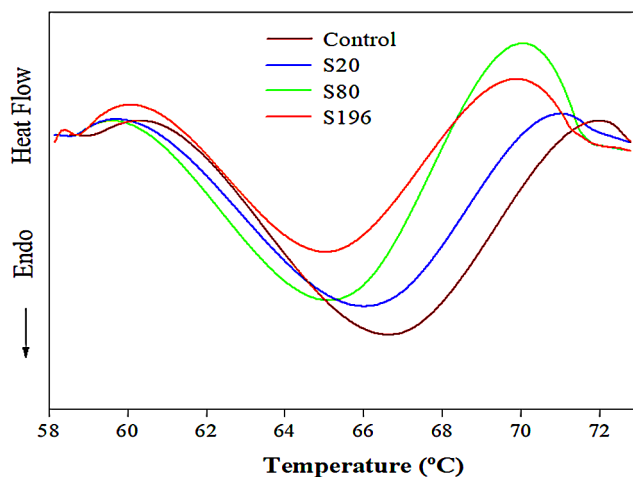
Fig. 3 Adzuki bean starch gelatinization curves: Control is starch gelatinized by heat-moisture (HMT), S20 is starch gelatinized by HMT and frozen at -20±2°C, S80 is starch gelatinized by HMT and frozen at -80±2°C and S196 is starch gelatinized by HMT and frozen at -196±3°C

surface" when the pores and channels connect with the particle's external surface [40]. In the case of hydrothermally treated starches by HMT, the specific surface area is minimal due to gelatinization. However, when stored at low temperatures, retrogradation occurs, leading to an increase in the number of voids shortly after drying.

De La Hera, Gomez, and Rosell [41], found that hydration properties are dependent on the specific surface area exposed, where water molecules bind to fine particles.

The lowest initial gelatinization temperatures (To) were observed for frozen starch samples, with S196 standing out (59.17 °C) (Table 3), where both samples showed significant differences. The same trend was observed for Tp and Tc (Fig. 3), where among the modified starches, S20 exhibited the highest values, 66.92 °C and 71.51 °C, respectively.

This can be explained as the slower freezing method results in a more stable and ordered structure for starch, which, in turn, requires higher temperatures and greater energy consumption for gelatinization [35]. Variations in crystalline form, crystalline size, degree of crystalline perfection, and the type of starch chain entanglement reflected the difference in gelatinization temperature [42].

The ΔH values were highest for the frozen starches compared to the control, with a value of 5.55 J g^{-1} for S20. This difference between the control and the cold-treated starches is due to macromolecule cleavage, causing rearrangement to form more double-helix structures [22]. An increase in ΔH represents that more energy is required to break the amylose-amylose and amylose-amylopectin chains [43]. According to Wei et al. [44], cooked and then frozen oatmeal cookies exhibited type A crystallinity and had an increase in Tp and
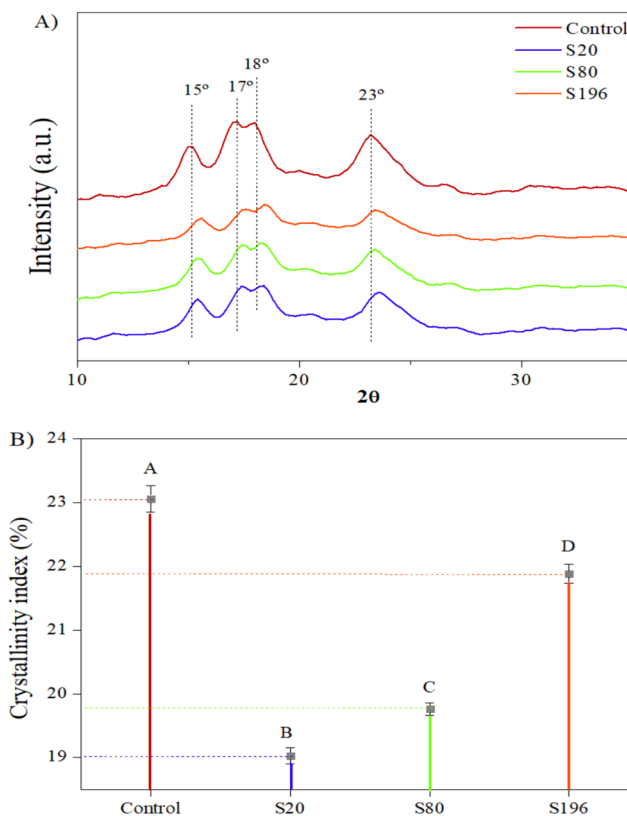
Fig. 4 X-ray diffraction patterns of bean starch: (**A**) diffractogram of 10–35° and (**B**) crystallinity index (%). Control is starch gelatinized by heat-moisture (HMT), S20 is starch gelatinized by HMT and frozen at -20±2°C, S80 is starch gelatinized by HMT and frozen at -80±2°C and S196 is starch gelatinized by HMT and frozen at -196±3°C

ΔH due to the double helix and the order of the helix structure of starch molecules.

Starch crystalline structure

The diffractograms of gelatinized and frozen starch are presented in Fig. 4A, where a doublet at 17° and 18° (2θ) and single peaks at 15° and 23° (2θ) were observed, consistent with the crystallinity of type A starch, as found in cereals by Ding et al. [45]. Regardless of the technique and temperature used, the crystalline form remained unchanged; only differences in crystallinity index were observed. This indicates that the type of crystallinity remained unaltered for starches subjected to both direct and indirect freezing, where starch retrogradation was not sufficient to shift the main peaks.

Yang et al. [34] also did not observe a change in the crystalline pattern even after 30 days of cold storage (-20 °C), but they noticed a reduction in crystallinity of 6.12%. The control sample had a crystallinity index value of 23.06% (Fig. 4B), which was higher than the other formulations. This was because freezing at a very slow rate, as in the case

of S20 and S80, caused more damage to the granule structure. Almeida et al. [25] found that red bean starch had a crystallinity ranging from 27.32 to 33.41%, and Maaran et al. [46] observed variations from 19.9 to 26.5% in starches obtained from different grain varieties. In this case, thermal modification (HMT + freezing) primarily affected the crystalline zones of the starch granules. Wei et al. [44] showed that the crystalline peaks of type A in cooked oat starch were destroyed by cryopreservation, resulting in lower crystallinity than the control, due to the steam cooking process causing damage such as granule rupture and debranching of the starch.

Short-range ordered structure of starch

The spectra of adzuki bean starch are shown in Fig. 5A, where the control starch exhibited more defined peaks, and it was not possible to detect the presence of new functional groups in the treated starches, only differences in intensity among the formulations, especially those stored at colder temperatures, such as S196. According to Wei et al. [44], the absorption peak intensity of cooked starch decreased after
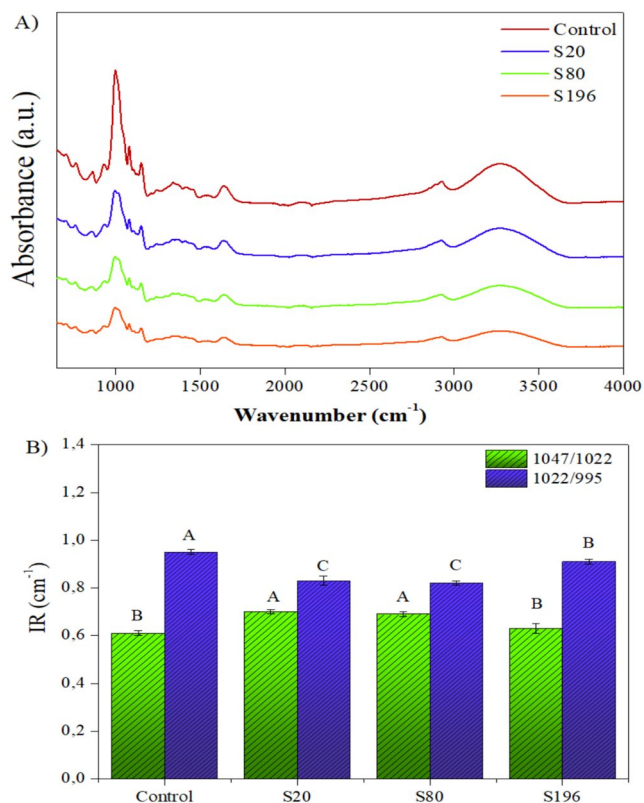
Fig. 5 Fourier transform infrared spectroscopy of starch modified by HMT + freezing: (**A**) Spectroscogram from 650–4000 cm^{-1} and (**B**) IR1047/1022 and IR1022/995. Control is starch gelatinized by heat-moisture (HMT), S20 is starch gelatinized by HMT and frozen at -20 ± 2ºC, S80 is starch gelatinized by HMT and frozen at -80 ± 2ºC and S196 is starch gelatinized by HMT and frozen at -196 ± 3ºC

freezing, indicating a weakening of the degree of short-chain order.

The peak around 3300 cm^{-1} corresponds to OH stretching vibration and hydrogen bond vibration, while the absorption peak at 2931 cm^{-1} is generated by CH stretching vibration, and the peak at 1625 cm^{-1} is associated with H-O bending vibration [47]. The most significant differences were found in the range of 650 to 1300 cm^{-1}, where the band at 995 cm^{-1} reflects the structure of hydrated starch, while 1047 cm^{-1} defines the crystalline zones and 1022 cm^{-1} the amorphous zones of starch granules, and the ratio between them provides an idea of the short-range ordered structure (Fig. 5B) [48]. Bands around 1002 cm^{-1} were attributed to COH bonds and were correlated with the amorphous state in starch [49].

There was no significant difference in the values of IR1047/1022 between S20 (0.70) and S80 (0.69), which had the highest values, as well as between the control (0.61) and S196 (0.63). Yang et al. [34] observed higher values of IR1047/1022 for type A starch after 8 weeks of cold storage (-20 °C). As for the IR1022/995 ratio, the control had the highest value (0.95) and showed a significant difference compared to the formulations subjected to freezing, where it can be seen that both S20 (0.83) and S80 (0.82) were similar, with values lower than the control, as well as S196 (0.91). This indicates that S196 had less mechanical damage to the starch crystalline structures after freezing/thawing. This difference is due to the freezing process, which reduces the content of amorphous substances, promotes internal reorganization of starch molecules, and consequently expands the short-range ordered structure, especially when carried out in short times [22].

The reduction in IR1022/995 is due to the significant damage caused to the sample's structure by the ice crystals formed during slow freezing (S20 and S80), where it facilitated the association of macromolecules and stimulated the formation of hydroxyl groups [50]. It was noted that the freezing rate influenced the crystalline structure of starch granules, strengthening progressively as the freezing rate increased.

Analysis of microstructure

The control starch granules presented small aggregates, as shown in Fig. 6A, due to adhesion mechanisms such as hydrogen bonding, Van der Waals interactions, and electrostatic forces resulting from HMT, where the surfaces were predominantly smooth and flat or slightly concave, sometimes even multifaceted. Observing the frozen formulations (Fig. 6B-D), it is evident that different freezing methods resulted in different surface damages. Therefore, the smaller the ice crystals (S20), the greater the damage to the starch

Fig. 6 Scanning electron microscopy of adzuki bean starch. (**A**) Control is starch gelatinized by heat-moisture (HMT), (**B**) S20 is starch gelatinized by HMT and frozen at -20±2ºC, (**C**) S80 is starch gelatinized by HMT and frozen at -80±2ºC and (**D**) S196 is starch gelatinized by HMT and frozen at -196±3ºC
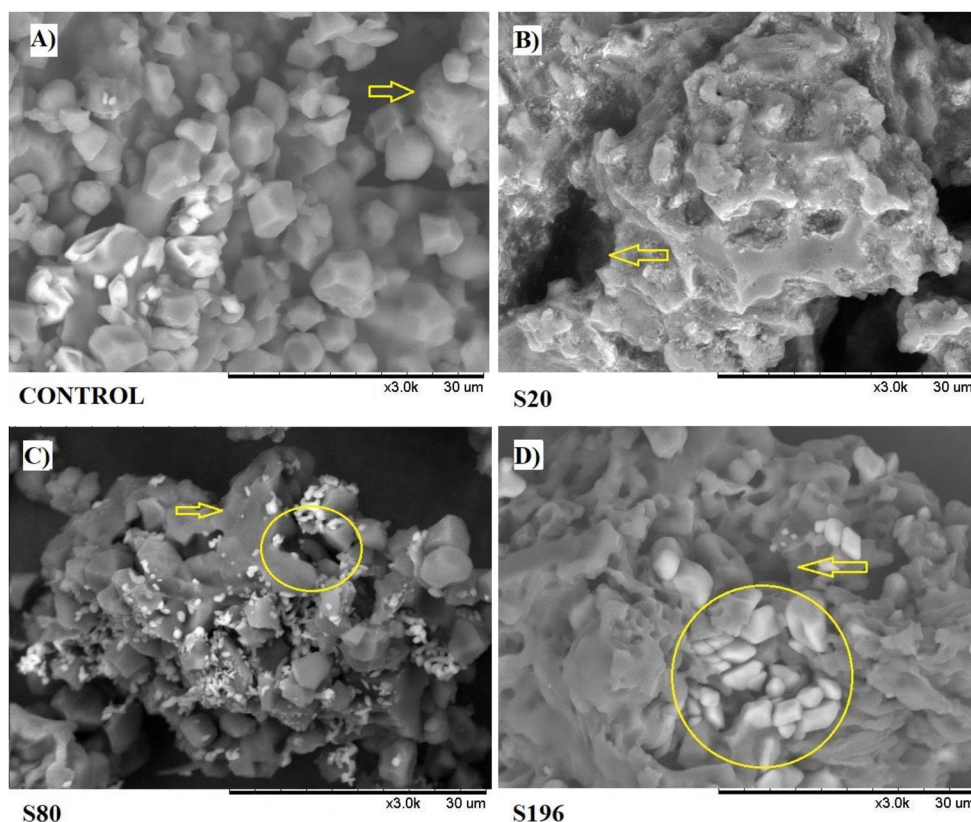
surface [51]. In Fig. 6B, the granules were gelatinized by HMT and did not withstand the temperature of -20 ºC (S20), where after retrogradation and drying of the starch, a narrowing of the granules and larger aggregates compared to the control was observed, making the geometry undefined. This trend was also confirmed for formulations S80, while in Fig. 6D, exposure to liquid nitrogen at -196 °C resulted in greater preservation in the center of the granules, leading to the formation of a gelatinized part around, with small cavities along the surface.

According to Wei et al. [27], small depressions and grooves were observed on the surface of frozen starches, and Yang et al. [34] found that the granular structure of corn starch was destroyed after freezing. The morphological changes indicated that the freezing process caused significant ruptures in the granular structures of the starch. This occurred due to expansion and pressure exerted by the ice matrix resulting from the freezable water fraction, which occupied the interior of the granule or its wall channels [52]. Wei et al. [44] found that for cooked oat starch, the surface is compact and continuous, and after freezing, the structure becomes brittle and the pore distribution is irregular, indicating that cooking followed by freezing is more destructive.

Conclusion

The results of this study provide new insights into the effect of freezing methods on the properties of initially heat-moisture-treated (HMT) adzuki bean starch. In comparison to S20 and S80, S196 had the highest freezing rate (1.21 °C/min), smaller particle sizes (21–27 µm), reduced solubility (4.13–4.71%), and increased swelling power (6.29–6.89 g g^{-1}), demonstrating that the application of liquid nitrogen modified the starch's hydration capacity. Furthermore, the results reveal that freezing conditions had a significant impact on starch digestibility, with the lowest glycemic index (GI) obtained in S20 (68.36). Faster freezing rates also increased the specific surface area of starch by up to 2.1 times compared to the control, which had a substantial effect on gelatinization properties. Regardless of the freezing temperature, the crystalline form (type A) remained unchanged, and no new functional groups were identified in the starches. Finally, scanning electron microscopy (SEM) confirmed the different surface damages caused by freezing. In summary, from a technological perspective, gelatinized adzuki bean starch frozen at -196 °C (S196) demonstrated high functionality for use in the development of frozen starch-based foods.

By combining freezing with HMT, we introduce a new approach to starch modification that may offer advantages

over simple methods. Utilizing combined thermal physical pre-treatments has the advantage of modifying native starch quickly without the use of chemical reagents, thus making it feasible for large-scale use due to the ease of the process. This study investigates the effect of heat when applied at temperatures sufficient for starch gelatinization, followed by the freezing step, while also highlighting that methods with higher freezing rates are less aggressive to the granular structure.

Author contributions **R.A**: Formal analysis, Methodology, Conceptualization, Writing – original draft. **N.C**: Writing – review & editing, Software. **I.F**: Methodology, Validation. **M.P**: Investigation. **J.F**: Writing – original draft. **R.E**: Funding acquisition, Resources. **V.F**: Validation. **T.P**: Software. **A.S**: Data curation, Visualization. **A.Q**: Writing – review and editing. **P.G**: Project administration.

Data availability Data will be made available on request.

Declarations

Competing interests The authors affirm that they do not have any known financial conflicts of interest or personal relationships that could have been perceived as influencing the research presented in this paper.

References

1. R.L.J. Almeida, N.C. Santos, W.B.B. Lima, C.E.A. Padilha, N.S. Rios, E.S. Santos, Int. J. Biol. Macromol. **222**, 65–76 (2022a). https://doi.org/10.1016/j.ijbiomac.2022.09.089

2. C. Cui, Y. Jia, M. Qi. Sun, N. Yu, L. Ji, Y. Dai, Y. Wang, L. Qin, Q. Xiong, Sun, Carbohydr. Polym. **291**, 119624 (2022). https://doi.org/10.1016/j.carbpol.2022.119624

3. F.A. Purwandari, C. Westerbos, K. Lee, V. Fogliano, E. Capuano, Food Res. Int. **170**(112956) (2023). https://doi.org/10.1016/j.foodres.2023.112956

4. Z. Shi, Y. Yao, Y. Zhu, G. Ren, Food Agric. Immunol. **28**, 78–89 (2017). https://doi.org/10.1080/09540105.2016.1208152

5. R.L.J. Almeida, N.C. Santos, J.V.F. Feitoza, G.M. Silva, C.E.S. Sousa, R.S. Eduardo, M.M.A. Mota, Carbohydr. Polym. Technol. Appl. **3**, 100192 (2022b). https://doi.org/10.1016/j.carpta.2022.100192

6. E.B.M. Viana, N.L. Oliveira, J.S. Ribeiro, M.F. Almeida, C.C.E. Souza, J.V. Resende, L.S. Santos, C.M. Veloso, Food Packaging Shelf Life. **31**, 100776920 (2022). https://doi.org/10.1016/j.fpsl.2021.100776

7. H. Wang, Y. Zhang, P. Su, N. Pan, X. Liu, Y. Zhang, H. Zhang, J. Cereal Sci. **112**, 103704 (2023). https://doi.org/10.1016/j.jcs.2023.103704

8. T. Chu, T.J. Shi, Y. Xia, H. Wang, G. Fan, M. Yang, Ind. Crops Prod. **187**, 115327 (2022). https://doi.org/10.1016/j.indcrop.2022.115327

9. R. Jia, C. Cui, L. Gao, Y. Qin, N. Ji, L. Dai, Y. Wang, L. Xiong, R. Shi, Q. Sun, Carbohydr. Polym. **321**, 121260 (2023). https://doi.org/10.1016/j.carbpol.2023.121260

10. K. Kunyanee, N. Luangsakul, LWT. 154,112694 (2022) https://doi.org/10.1016/j.lwt.2021.112694

11. J.J. Park, I.F. Olawuyi, W.Y. Lee, Int. J. Biol. Macromol. **153**, 215–223 (2020). https://doi.org/10.1016/j.ijbiomac.2020.02.331

12. K. Schafranski, V.C. Ito, L.G. Lacerda, Food Hydrocoll. **117**, 106690 (2021). https://doi.org/10.1016/j.foodhyd.2021.106690

13. B.R. Chen, Y.X. Teng, L.H. Wang, F.Y. Xu, Y. Li, Q.H. Wen, R. Wang, J. Li, Z. Wang, X.A. Zeng, Int. J. Biol. Macromol. **231**, 123085 (2023). https://doi.org/10.1016/j.ijbiomac.2022.12.304

14. X. Cheng, M. Zhang, B. Xu, B. Adhikari, J. Sun, Ultrason. Sonochem. **27**, 576–585 (2015). https://doi.org/10.1016/j.ultsonch.2015.04.015

15. B.A. Anderson, S. Sun, F. Erdogdu, R.P. Singh, Int. J. Refrig. **27**(1), 63–72 (2004). https://doi.org/10.1016/S0140-7007(03)00093-8

16. W. Gao, Y. Huang, X.A. Zeng, M.A. BrennanInt, J. Biol. Macromol. **135**, 839–844 (2019). https://doi.org/10.1016/j.ijbiomac.2019.05.186

17. B. Gong, M. Xu, B. Li, H. Wu, Y. Liu, G. Zhang, S. Ouyang, W. Li, Food Res. Int. **102**, 776–784 (2017). https://doi.org/10.1016/j.foodres.2017.09.078

18. H.T. Li, W. Zhang, Y. Chen, Y. Pan, Y. Bao, Food Chem. (2023). https://doi.org/10.1016/j.foodchem.2023.136344. 424,136344

19. L. Han, S. Cao, Y. Yu, X. Xu, X. Cao, W. Chen, Food Chem. (2021). https://doi.org/10.1016/j.foodchem.2021.129929. 360,129929

20. Y. Guo, T. Xu, N. Li, Q. Cheng, D. Qiao, B. Zhang, S. Zhao, Q. Huang, Q. Lin, Int. J. Biol. Macromol. **135**, 437–444 (2019). https://doi.org/10.1016/j.ijbiomac.2019.05.189

21. S. Zhang, Q. Li, Y. Zhao, Z. Qin, M. Zheng, H. Liu, J. Liu, Food Chem. X. **15**, 100410 (2022). https://doi.org/10.1016/j.fochx.2022.100410

22. Q. Wang, L. Li, X. Zheng, Food Chem. **344**, 128700 (2020). https://doi.org/10.1016/j.foodchem.2020.128700

23. S. Mizrahi, Woodhead Publishing. 324–348 (2010). https://doi.org/10.1533/9781845699260.2.324

24. R.L.J. Almeida, T.S. Pereira, V.A. Freire, Â.M. Santiago, H.M.L. Oliveira, L.S. Conrado, R.P. Gusmão, Int. J. Biol. Macromol. **141**, 1210–1219 (2019). https://doi.org/10.1016/j.ijbiomac.2019.09.072

25. R.L.J. Almeida, N.C. Santos, G.M. Silva, J.V.F. Feitoza, V.M.A. Silva, V.H.R. Alcântara, R.E. Silva, C.E.S. Muniz, J. Food Process. Eng. 45, 13994 (2022c). https://doi.org/10.1111/jfpe.13994

26. Y. Yang, S. Zheng, Z. Li, Z. Pan, Z. Huang, J. Zhao, Z. Ai, Food Hydrocoll. **115**, 106619 (2021). https://doi.org/10.1016/j.foodhyd.2021.106619

27. Q. Wei, G. Zhang, J. Mei, C. Zhang, J. Xie, J. Int. J. Biol. Macromol. **240**, 124424 (2023). https://doi.org/10.1016/j.ijbiomac.2023.124424

28. K.N. Jan, O.S. Panesar, J.C. Rana, S. Singh, Int. J. Biol. Macromol. **102**, 315–322 (2017). https://doi.org/10.1016/j.ijbiomac.2017.04.027

29. Z. Han, Y. Han, J. Wang, Z. Liu, R. Buckow, J. Cheng, J. Food Process. Preserv. **44**(3), 14353 (2020). https://doi.org/10.1111/jfpp.14353

30. J. Tian, Y. Cai, W. Qin, Y. Matsushita, X. Ye, Y. Ogawa, Food Chem. **257**, 23–28 (2018). https://doi.org/10.1016/j.foodchem.2018.03.005

31. G.L. Miller, Anal. Chem. **31**(3), 426–428 (1959). https://doi.org/10.1021/ac60147a030

32. W. Yu, D. Xu, H. Zhang, H.L. Guo, T. Hong, W. Zhang, X. Xu, Food Hydrocoll. (2020). https://doi.org/10.1016/j.foodhyd.2019.105591. 102,105591

33. Z. Zhu, Q. Zhou, Q.D.W. Sun, Trends Food Sci. Technol. **90**, 13–25 (2019). https://doi.org/10.1016/j.tifs.2019.05.012

34. Z. Yang, W. Yu, D. Xu, L. Guo, F. Wu, X. Xu, Carbohydr. Polym. (2019). https://doi.org/10.1016/j.carbpol.2019.115142. 223,115142

35. H. Tao, P. Wang, F. Wu, Z. Jin, X. Xu, RSC Adv. **6**(100), 97907–97911 (2016). https://doi.org/10.1039/C6RA11287K

36. X. Ren, J. Chen, C. Wang, M.M. Molla, X. Diao, Q. Shen, J. Cereal Sci. **69**, 166–173 (2016). https://doi.org/10.1016/j.jcs.2016.03.007

37. F. Jiang, C. Du, Y. Guo, J. Fu, W. Jiang, S. Du, S Food Hydrocoll. (2020). https://doi.org/10.1016/j.foodhyd.2019.105515. 101,105515

38. Y. Xu, C. Wang, X. Fu, Q. Huang, B. Zhang, Food Hydrocoll. **76**, 96–102 (2018). https://doi.org/10.1016/j.foodhyd.2017.02.015

39. S.R. Kumar, N. Tangsrianugul, M. Suphantharika, Foods. **12**(12), 2413 (2023). https://doi.org/10.3390/foods12122413

40. R. Digaitis, P. Falkman, P.V. Oltner, L.E. Briggner, V. Kocherbitov, V Carbohydr. Polym. **291**, 119542 (2022). https://doi.org/10.1016/j.carbpol.2022.119542

41. L.E. Hera, M. Gomez, C.M. Rosell, Carbohydr. Polym. **98**(1), 421–427 (2012). https://doi.org/10.1016/j.carbpol.2013.06.002

42. B. Wei, X. Hu, B. Zhang, H. Li, X. Xu, Z. Jin, Y. Tian, Int. J. Biol. Macromol. **62**, 652–656 (2013). https://doi.org/10.1016/j.ijbiomac.2013.10.008

43. L. Jayakody, R. Hoover, Food Res. Int. **35**(7), 665–680 (2002). https://doi.org/10.1016/S0963-9969(01)00204-6

44. X. Wei, Y. Gong, X. Hu, LWT. **167**, 113839 (2022). https://doi.org/10.1016/j.lwt.2022.113839

45. L. Ding, B. Zhang, C.P. Tan, X. Fu, Q. Huang, Int. J. Biol. Macromol. **137**, 1068–1075 (2019). https://doi.org/10.1016/j.ijbiomac.2019.06.226

46. S. Maaran, R. Hoover, E. Donner, Q. Liu, Food Chem. **152**, 491–499 (2014). https://doi.org/10.1016/j.foodchem.2013.12.014

47. C. Zhong, Y. Xiong, H. Lu, S. Luo, J. Wu, J. Ye, C. Liu, LWT. **154**, 112890 (2022). https://doi.org/10.1016/j.lwt.2021.112890

48. L.C. González, M.A. Loubes, M.M. Bertotto, R.I. Baeza, M.P. Tolaba, Carbohydr. Polym. Technol. Appl. **2**, 100168 (2021). https://doi.org/10.1016/j.carpta.2021.100168

49. I.A. Wani, M. Jabeen, H. Geelani, F.A. Masoodi, I. Saba, S. Muzaffar, Food Hydrocoll. **35**, 253–263 (2014). https://doi.org/10.1016/j.foodhyd.2013.06.002

50. S. Meziani, J. Jasniewski, C. Gaiani, I. Ioannou, J.M. Muller, M. Ghoul, S. Desobry, J. Food Eng. **107**(3–4), 358–365 (2011). https://doi.org/10.1016/j.jfoodeng.2011.07.003

51. G. Petzold, J.M. Aguilera, Food Biophys. **4**, 378–396 (2000). https://doi.org/10.1007/s11483-009-9136-5

52. H. Wang, K. Xu, X. Liu, Y. Zhang, X. Xie, H. Zhang, Food Hydrocoll. **111**(106168), 92021 (2021a). https://doi.org/10.1016/j.foodhyd.2020.106168